Nuclear Physics B257 [FS14] (1985) 173–198

NUMERICAL SOLUTION OF FIELD THEORIES USING RANDOM WALKS

T. BARNES*

Theory Group, HEP Division, Rutherford Appleton Laboratory, Chilton, Didcot, Oxon OX11 OQX, UK

G.J. DANIELL

Department of Physics, University of Southampton, Highfield, Southampton, Hants SO9 5NH, UK

Received 12 November 1984

We show how random walks in function space can be employed to evaluate field theoretic vacuum expectation values numerically. Specific applications which we study are the two-point function, mass gap, magnetization $\langle\phi\rangle$ and classical solutions.

This technique offers the promise of faster calculations using less computer memory than current methods.

1. Introduction

It is well known that the Schrödinger equation, written in euclidean time, $\tau = it$, becomes a diffusion equation. This suggests that a computer simulation of the process of diffusion may be a useful technique for obtaining numerical solutions to quantum mechanical problems. A suitable model of diffusion is provided by a random walk.

In this paper we establish a relation between path integrals and random walks in quantum mechanics and quantum field theories, and we show that random walks can be used as an alternative to the well-known Monte Carlo method for numerical calculations on these problems.

The details of the paper are as follows: in sect. 2 we show how random walks may be used to follow the evolution of a quantum mechanical state in euclidean time. The effect of potential energy is included by allowing the absorption of random walks. The application of the technique to quantum mechanics described in this section is illustrated with numerical results for a SHO potential.

* Address from January 1985: Department of Physics, University of Toronto, Toronto, Ontario, M5S 1A7, Canada.

In sect. 3 we extend the quantum mechanical technique to field theories, using a scalar field in one space dimension for our discussion. The practical application of random walks to systems with many degrees of freedom is shown to be feasible provided we allow the creation of new random walks as branches, to compensate for the absorption of the walks. We develop an elegant modification that enables vacuum matrix elements to be easily evaluated and discuss computational techniques.

Sect. 4 gives some applications of the random walk method to nontrivial problems, specifically the evaluation of Green functions, mass gaps, mean fields and classical solutions. For illustration here we use both the free massive scalar theory and the model $\lambda{:}(\phi^6 - \phi^4){:}$. The mass gap of the latter model has previously been measured on a lattice using hamiltonian methods, and we show that the mass gap obtained using random walks is generally in good agreement with the earlier results.

We conclude with suggestions for the future development and application of this technique.

As our application of random walks to calculating matrix elements has some relation to existing literature, we here review the connection of this paper to these earlier contributions.

There is a close resemblance between our random walk method and two lines of development which have appeared in the literature, both of which derive from the quantum mechanical applications of random walks due to Kalos et al. [1–3]. All three field theoretic methods have in common the use of random walks in function space to generate the vacuum state, with the creation and absorption of branch walks to simulate the effect of a potential or a related weight function.

The Green function Monte Carlo (GFMC) method employed by Heys and Stump [4] uses random walks to iterate an integral equation for the vacuum state $\psi_0[A]$ which is derived from the functional Schrödinger equation. Applications of the GFMC method to SU(2) and U(1) gauge theories and the XY model have appeared in the literature.

A second approach is the guided random walk (GRW) method of Chin, Koonin, Negele and Serot [5]. This method is more closely related to our work, in that it creates and destroys walks with an amplitude obtained directly from $V(\phi) - E$, just as we have done. One important difference is the use of a gaussian distribution of step sizes in the GRW technique, obtained from a solution of the free diffusion equation. In contrast, we change the field by a small fixed step, and do not need to compute a solution of the diffusion equation. This should be substantially faster and we anticipate that it will also be advantageous in applications to gauge theories with complicated group spaces and in fermionic random walks.

A crucial feature which distinguishes the methods is the weight with which configurations are generated. Of the three techniques, our approach alone generates configurations with the correct vacuum state probability $|\psi_0[\phi]|^2$. Both the GFMC and GRW approaches require a vacuum state ansatz $\Phi_0[\phi]$ as input, and their

matrix elements are generally only correct when this ansatz is exactly equal to the true vacuum state. Chin et al. [5] note that this ansatz dependence may be turned into an advantage, in that one may develop an understanding of the vacuum state from various trial vacuua. It is clear that our method, which automatically generates the correct vacuum matrix elements, may prove superior in problems having a vacuum state which is poorly understood, complicated or difficult to model.

Finally, we note that there are a number of other stochastic approaches to finding low-lying eigenstates of the hamiltonian [6,7] without following the evolution of states in euclidean time as we have done here.

2. Random walks and quantum mechanics

2.1. A RELATION BETWEEN PATH INTEGRALS, RANDOM WALKS AND THE SCHRÖDINGER EQUATION

In this section we consider quantum mechanical systems in one space dimension and euclidean time. The wave function satisfies

$$-\frac{\partial\psi}{\partial\tau}=-\frac{1}{2}\frac{\partial^2\psi}{\partial x^2}+V(x)\psi. \tag{2.1}$$

A computer simulation of diffusion using a random walk can be generated as follows.

Consider a set of equally spaced sites labelled by j along the x-axis, and suppose that a particle, initially at $j=0$, has probability $\frac{1}{2}$ of stepping either to the right or to the left by one site at each time step. Such a lattice is shown in fig. 1. Let $p(j,n)$ be the probability that the particle is at site j after n steps. If the particle is at site j after $n+1$ steps, then it must have been at $j\pm1$ after n steps, so $p(j,n)$ clearly satisfies

$$p(j,n+1)=\tfrac{1}{2}\left[p(j-1,n)+p(j+1,n)\right]. \tag{2.2}$$

The analytic solution of this recurrence relation is

$$p(j,n)=2^{-n}n!/\left[\left(\tfrac{1}{2}(n-j)\right)!\left(\tfrac{1}{2}(n+j)\right)!\right], \tag{2.3}$$

and approximate numerical values of p could be obtained, as a histogram, by following the evolution of a large number of walks through n steps in a computer simulation and counting the fraction that end at site j.

If n is large, $p(j,n)$ does not vary rapidly with j or n, so we can regard the numbers $p(j,n)$ as samples of a function $p(x,\tau)$ of continuous space and time variables at the points $x=jh_x$ and $\tau=nh_\tau$, and p satisfies

$$p(x,\tau+h_\tau)=\tfrac{1}{2}\left[p(x-h_x,\tau)+p(x+h_x,\tau)\right]. \tag{2.4}$$

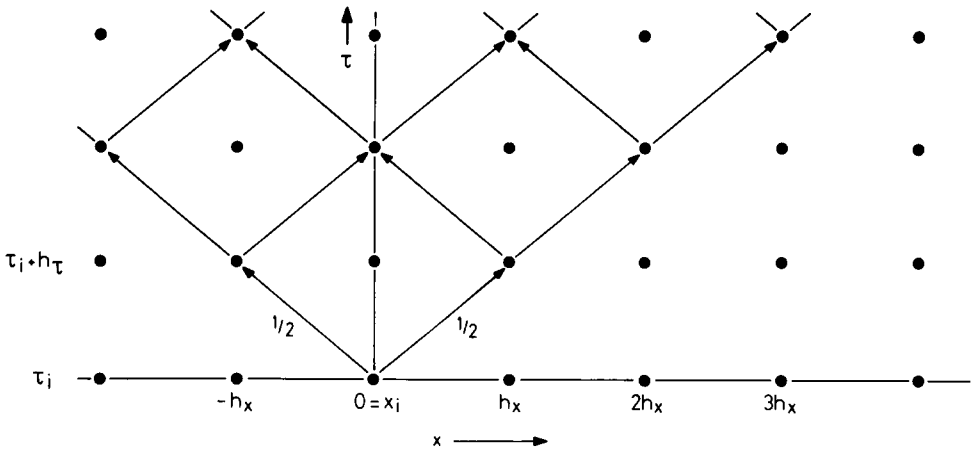

Fig. 1. Possible random steps on the (x, τ) lattice.

In the continuum limit $h_x \to 0$, $h_\tau \to 0$, this becomes the differential equation

$$\frac{\partial p}{\partial \tau} = \frac{1}{2}\frac{h_x^2}{h_\tau}\frac{\partial^2 p}{\partial x^2}. \tag{2.5}$$

If we impose a constraint on our space and time lattice spacings so that in appropriate units $h_x^2 = h_\tau$, this is the Schrödinger equation for a free particle. The wave function at (x, τ) is equal, apart from a normalisation constant, to the probability that a random walk reaches x at time τ.

We note in passing that the solution of (2.5) corresponding to the boundary condition of starting at $x = 0$ at $\tau = 0$ is

$$p(x, \tau) = \left(2\pi h_x^2 \tau / h_\tau\right)^{-1/2} \exp\left[-x^2 h_\tau / 2h_x^2 \tau\right], \tag{2.6}$$

which could also be obtained from the asymptotic form of (2.3) for large n. We also note that the end points, x, of random walks have a gaussian distribution and this offers a possible method of generating random numbers with such a distribution.

A better known approach to the problem is that of Creutz and Freedman [8] who start with the Feynman path integral in euclidean time. Feynman and Hibbs [9] express the amplitude for a particle to go from $(0,0)$ to (x, τ) as a weighted sum over *all* paths from 0 to x, and the weight in the discrete time approximation is

$$W = \exp\left\{ -\sum_n \left(\frac{(x_{n+1} - x_n)^2}{2\varepsilon} + \varepsilon V(x_n) \right) \right\}. \tag{2.7}$$

The wave function for the free particle starting from (0,0) can be expressed as

$$\psi(x_N,\tau)=\eta\int_{-\infty}^{\infty}\prod_{n=1}^{N-1}\mathrm{d}x_n\exp\left\{-\frac{(x_{n+1}-x_n)^2}{2\varepsilon}\right\}. \tag{2.8}$$

Creutz and Freedman describe the evaluation of such multidimensional integrals by the Monte Carlo technique. This involves picking a set of points $x_1, x_2 \ldots x_{N-1}$ at random with uniform probability density. Because of the large variations in weight (2.7) it is much more efficient to pick a set of x_n with probability given by (2.7), and to weight all such sets equally. This is known as importance sampling and can be achieved in various ways such as the Metropolis or heat-bath algorithms described by Creutz and Freedman.

A further refinement is possible. Given x_n, x_{n+1} has a gaussian distribution, and as suggested above a suitable x_{n+1} could be generated using a random walk. We introduce intermediate time steps within the interval ε with separation $h_\tau \ll \varepsilon$, and a discrete lattice of x points with separation $h_x \ll x_{n+1}-x_n$. The paths used by Creutz and Freedman in the evaluation of the Feynman integral, when importance sampling is used, are then just random walks on this finer lattice of space and time points. There is in fact a difference in the boundary conditions: the paths used by Creutz and Freedman are constrained at both ends whereas ours may finish at any point. This is amplified later in subsect. 2.4; for the purpose of the present argument assume that paths generated sequentially as described are to be rejected unless they end at x. This discussion shows that, for a free particle, $\psi(x,\tau)$ which was written as a *weighted* sum over *all paths* from 0 to x, can also be written as an *unweighted* sum over *all random walks* from 0 to x.

We have had to use a time step, h_τ, which is defined to be much less than ε, but as the details on time scales less than ε cannot be very important, we claim that h_τ can be made as large as ε without worsening the approximation already implied by the introduction of steps of ε. The numerical results of the later sections show that a comparatively large value of h_τ is quite acceptable. Since $h_x = h_\tau^{1/2}$, this implies that $(x_{n+1}-x_n)^2/\varepsilon \sim 1$; surprisingly, this very coarse space lattice leads to no serious deterioration in the accuracy of the results.

To summarise: the wave function describing the evolution in euclidean time of a free particle can be calculated by using random walks starting at $x=0$ and stepping equally likely to the right or the left for the required time, and counting how often they end at point x.

2.2. INCLUSION OF A POTENTIAL $V(x)$

Everything so far has dealt with the motion of a free particle. There are several ways in which potential energy can be included in the random walk formalism. The simplest is to regard the random walk as a technique for generating paths with a

weight corresponding to the kinetic term in (2.7) and to calculate the contribution of the potential energy to the weight explicitly by

$$W_V = \exp\left\{ - \int V(x(\tau))\, \mathrm{d}\tau \right\}. \tag{2.9}$$

The path over which this integral is evaluated is just a random walk as described above.

A few numerical experiments show that, whereas this works well for quantum mechanics, when applied to field theory almost all paths acquire a negligible weight. Some technique is required which preferentially generates random walks for which the weight is appreciable, just as the random walks themselves are a subset of all possible paths, whose members tend to make appreciable contributions to the path integral.

An alternate approach which is explored in detail in this paper starts by assuming that *the random walk has a nonzero probability* $a(x)$ *of being absorbed* before each step. The recurrence relation then becomes

$$p(x, \tau + h_\tau) = (1 - a(x)) \tfrac{1}{2} \left[p(x - h_x, \tau) + p(x + h_x, \tau) \right], \tag{2.10}$$

with the continuum limit

$$\frac{\partial p}{\partial \tau} = \frac{1}{2} \frac{h_x^2}{h_\tau} \frac{\partial^2 p}{\partial x^2} - \frac{a(x) p}{h_\tau}. \tag{2.11}$$

This becomes the Schrödinger equation as before if we require that the probability $a(x)$ of a walk being absorbed at x is related to the potential $V(x)$ by $a(x) = h_\tau V(x)$. When a random walk is absorbed it is abandoned and a new walk is started from the origin. Thus far this approach offers no apparent advantage over the simple weighting using (2.9), but its superiority lies in the possibility of creating new walks. This is explained in sect. 3.

Any square-integrable solution to (2.1) can be written in terms of the eigenfunctions $\psi_n(x)$:

$$\psi(x, \tau) = \sum_n c_n \mathrm{e}^{-E_n \tau} \psi_n(x). \tag{2.12}$$

Therefore whatever the starting point, providing the ground state is not degenerate, the probability of the random walk reaching point x at very large τ approaches

$$\lim_{\tau \to \infty} \psi(x, \tau) = c_0 \mathrm{e}^{-E_0 \tau} \psi_0(x). \tag{2.13}$$

We may therefore obtain ground-state energies by

$$E_0 = - \frac{1}{\Delta \tau} \ln \left\{ \lim_{\tau \to \infty} p(\tau + \Delta \tau)/p(\tau) \right\}, \tag{2.14}$$

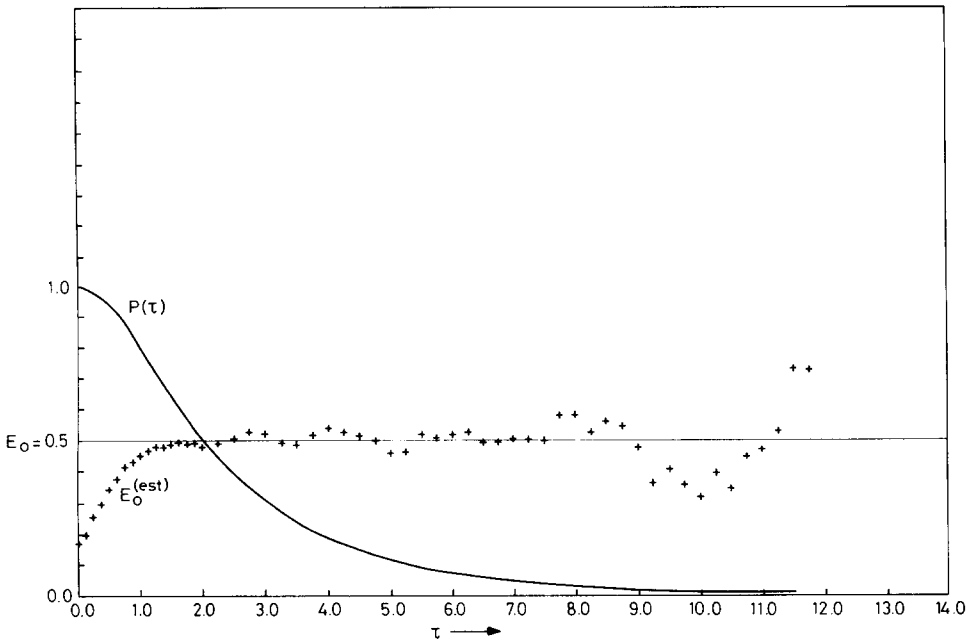

Fig. 2. Evaluation of the SHO ground-state energy using random walks.

where

$$p(\tau) = \sum_x p(x, \tau). \tag{2.15}$$

This method was apparently first suggested by Fermi [10]. It involves repeatedly evolving random walks from an initial point at $\tau = 0$ until we have determined $p(\tau)$ to the required accuracy, bearing in mind the statistical fluctuations. We can also obtain the ground-state wave function by evolving random walks from $(0,0)$ to a fixed large τ, and noting the arrival points x at τ. These have a probability distribution $p(x)$ which is proportional to $\psi_0(x)$.

As a specific example, consider the simple harmonic oscillator potential $V(x) = \frac{1}{2}x^2$. The fraction $p(\tau)$ of an initial 10^4 random walks which, having started at $(0,0)$ survive to time τ, is shown in fig. 2, together with the estimate of E_0 calculated by

$$E_0^{(\mathrm{est})} = -\frac{1}{\Delta\tau}\ln\{\, p(\tau + \Delta\tau)/p(\tau)\}. \tag{2.16}$$

The approach to the correct value $E_0 = 0.5$ is evident. In these calculations we have

taken $h_\tau = h_x^2 = \frac{1}{16}$ and $\Delta\tau = 10h_\tau$. The "equilibration time" τ_e during which the contamination of the wave function by contributions from excited states is reduced by a factor $1/e$ is $(E_m - E_0)^{-1}$. Here E_m is the lowest excited state occurring in the expansion (2.12). In our example the state $\psi_1(x)$ has a node at $x = 0$ and is not needed to describe a random walk starting at this point. The first level excited is $\psi_2(x)$, so $E_m = \frac{5}{2}$ and the equilibration time is $(E_2 - E_0)^{-1} = 0.5$. The approach of the estimate to the correct energy in fig. 2 is consistent with this value. We must follow the walks for several equilibration times to obtain a good estimate of E_0.

2.3. ACCURACY OF RANDOM WALK RESULTS

The increasing fluctuations at large values of τ in fig. 2 arise from the very small number of walks surviving for this long time. There is therefore an optimum time to measure E_0 when the errors due to contamination from excited states and due to statistical fluctuations are approximately equal. Estimates of these errors are

$$\frac{\delta E_0}{E_0} \sim e^{-(E_m - E_0)\tau}, \tag{2.17}$$

$$\frac{\delta E_0}{E_0} \sim N_\tau^{-1/2} \sim N_0^{-1/2} e^{E_0\tau/2}. \tag{2.18}$$

The minimum total error occurs at a time

$$\tau_{\text{opt}} \sim \frac{\ln(N_0)}{2E_m - E_0} \sim \frac{\ln(E_0/\delta E_0)}{E_m - E_0}, \tag{2.19}$$

and the number of initial random walks N_0 required to achieve an accuracy δE_0 in measuring E_0 is

$$N_0 \sim \left(\frac{E_0}{\delta E_0}\right)^{[2 + E_0/(E_m - E_0)]}. \tag{2.20}$$

For the results of fig. 2 with $N_0 = 10^4$ these equations imply that we can determine E_0 to an accuracy of about 2% at the optimum time $\tau_{\text{opt}} = 2$. Examination of fig. 2 supports these estimates. For $\tau \lesssim \tau_{\text{opt}}$ there is still extensive contamination of the ground state by higher excited states, and for $\tau \gtrsim \tau_{\text{opt}}$ the fluctuations due to worsening statistics grow rapidly larger.

Finally, to demonstrate that we can indeed generate $\psi_0(x)$ as well as E_0 using random walks, in fig. 3 we show a histogram of the arrival coordinates x of the 5053 random walks which survived to $\tau_{\text{opt}} = 2$. For each bin we plot the estimate of the probability of arriving in that bin divided by the bin width of $2h_x = 0.5$. For comparison the equivalently normalised continuum ground-state wave function $[1/(2\pi)^{1/2}]\exp(-\frac{1}{2}x^2)$ is also shown and agreement between these is clear.

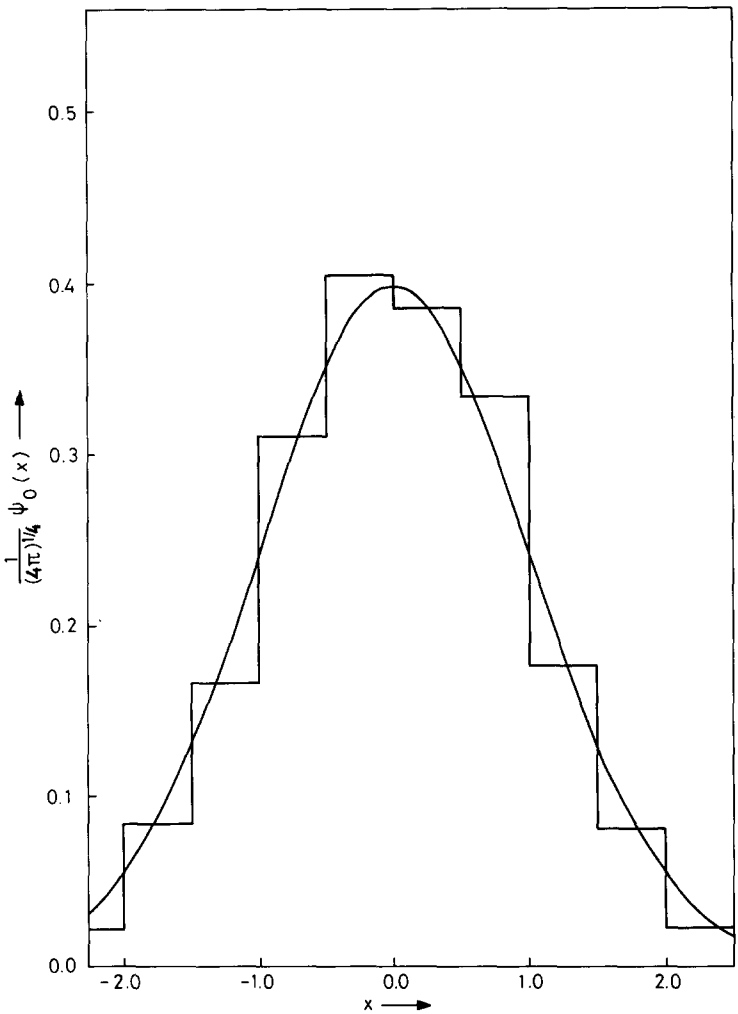

Fig. 3. The SHO ground-state wave function generated by random walks.

2.4. GENERATION OF $|\psi_0(x)|^2$ USING RANDOM WALKS

The calculation of matrix elements is obviously important. This cannot be done by just averaging the appropriate quantity over different random walks, since the probability of reaching x is proportional to $\psi_0(x)$ and not $|\psi_0(x)|^2$. This is in contrast to the technique described by Creutz and Freedman using the Metropolis or other algorithms where the probability of a path passing through a point x is proportional to $|\psi_0(x)|^2$. The essential difference between the approaches is that

Creutz and Freedman generate the whole path at once and there is no preferred time direction. Fortunately, there is a simple modification of the random walk technique which generates $|\psi_0(x)|^2$, which we shall illustrate in the context of quantum mechanics.

The Green function for the Schrödinger equation (2.1) may be written in an eigenmode expansion as

$$G(x_1, \tau_1; x_2, \tau_2) = \sum_n e^{-E_n(\tau_2 - \tau_1)} \psi_n^*(x_1) \psi_n(x_2), \tag{2.21}$$

and G may be identified with the probability of a random walk, starting at (x_1, τ_1), arriving at (x_2, τ_2). For sufficiently large $\tau_2 - \tau_1$, G satisfies

$$G(x_1, \tau_1; x_2, \tau_2) \sim e^{-E_0(\tau_2 - \tau_1)} \psi_0^*(x_1) \psi_0(x_2). \tag{2.22}$$

Suppose we calculate the probability $q(x, \tau)$ that a random walk which starts at $(0,0)$ survives to (x, τ), and thence to *any* y at 2τ. This is given by

$$q(x, \tau) = \int G(0,0; x, \tau) G(x, \tau; y, 2\tau) \, dy, \tag{2.23}$$

which for large τ is

$$\lim_{\tau \to \infty} q(x, \tau) = e^{-2E_0\tau} |\psi_0(x)|^2 \psi_0^*(0) \int \psi_0(y) \, dy. \tag{2.24}$$

If we normalise the resulting $q(x, \tau)$ to unity we obtain $|\psi_0(x)|^2$ directly. As an explicit example, recall the sequence of 10^4 random walks used to produce the results presented in figs. 2 and 3. If we calculate $|\psi_0(x)|^2$ with this same sequence of walks, using the algorithm described above and taking $\tau = 2.0$, the 1817 random walks which survived to $2\tau = 4.0$ generate the $|\psi_0(x)|^2$ shown in fig. 4. Agreement between the histogram and the exact result $|\psi_0(x)|^2 = e^{-x^2}/\sqrt{\pi}$ is clearly in evidence.

Expectation values for the ground state can now be calculated as follows. We start a random walk from $(0,0)$ and continue for a long time τ so that the excited states have decayed away. There we *note* the value of the appropriate operator but do not yet use this value. The walk is then continued for another period τ. If the walk survives this *without being absorbed*, the previously noted value of the operator is included in an average. After many such walks this average approaches the appropriate matrix element.

We note in passing that there is a related technique for generating $|\psi_0|^2$ in the integral equation technique due to Kalos [2].

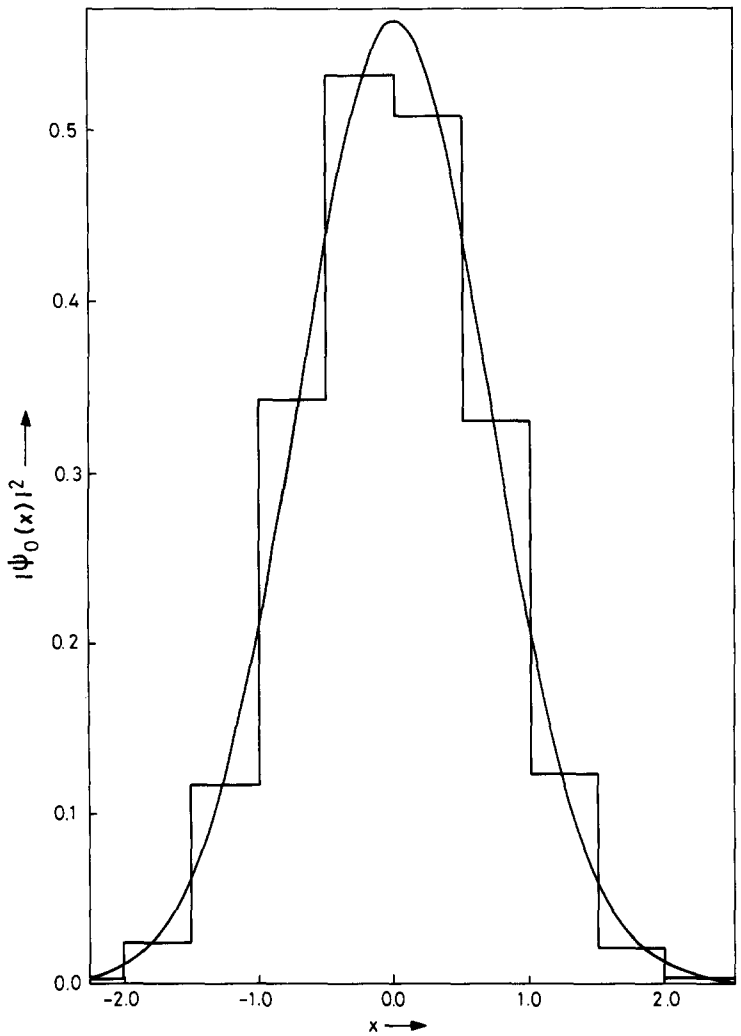

Fig. 4. The SHO ground-state probability density $|\psi_0(x)|^2$ generated by random walks.

3. Random walks and quantum fields

3.1. GENERATION OF THE VACUUM STATE $\psi_0[\phi(x)]$ AND E_0

We may use random walks in function space to solve lattice quantum field theories analogously to the previously discussed application to quantum mechanics. Some modification of the procedure is necessary due to the longer equilibration time τ_e relative to the lattice time step h_τ for many degrees of freedom, and also because we are more interested in expectation values than in the ground-state energy.

For illustrative purposes we first consider a free scalar field theory. We wish to generate the ground-state wave functional $\psi_0[\phi(x)]$, following which we may evaluate the expectation value of any operator or function of the field*, $O(\phi(x))$, as

$$\langle 0|O|0\rangle = \int \mathrm{D}\phi\, \psi_0^*[\phi(x)]\, O(\phi(x))\, \psi_0[\phi(x)]\,. \tag{3.1}$$

To find $\psi_0[\phi]$ we again establish a connection between the Schrödinger equation for ψ and random walks. In euclidean time a wave functional $\psi[\phi(x)]$ satisfies the Schrödinger equation [11]

$$-\frac{\partial\psi[\phi]}{\partial\tau} = \int \mathrm{d}x \left\{ -\frac{1}{2}\frac{\delta^2}{\delta\phi(x)^2} \underbrace{+\tfrac{1}{2}(\nabla\phi)^2 + \tfrac{1}{2}m^2\phi^2}_{V(\phi)\,=\,\text{classical energy density}} \right\} \psi[\phi], \tag{3.2}$$

This may be visualized as a diffusion equation for ψ in an infinite number of coordinates, $\{\phi(x)\}$. To evaluate $\psi_0[\phi(x)]$ numerically, we must restrict this space to a finite set of N coordinates $\{\phi(x_j) \equiv \phi_j\}$. The diffusion equation for $\psi(\phi_1, \phi_2 \ldots \phi_N, \tau)$ then becomes a partial differential equation in N dimensions:

$$-\frac{\partial\psi}{\partial\tau} = \sum_{j=1}^{N} \left\{ -\frac{1}{\nu}\frac{1}{2}\frac{\partial^2}{\partial\phi_j^2} + \nu\left(\tfrac{1}{2}(\nabla\phi)_j^2 + \tfrac{1}{2}m^2\phi_j^2\right) \right\} \psi\,. \tag{3.3}$$

Here ν is the unit cell volume, $\nu = h_x^S$ in S spatial dimensions. For convenience we refer to the set of $\{\phi_1, \phi_2 \ldots \phi_N\}$ coordinates which describe a given classical configuration on the lattice with a single ϕ rather than writing $(\phi_1, \phi_2 \ldots \phi_N)$ repeatedly. To solve (3.3) using random walks, we must restrict the continuous coordinates ϕ_j to discrete values. For each of the coordinates ϕ_j we allow values $0, \pm h_\phi, \pm 2h_\phi, \ldots$. A complete set of values for the $\{\phi_j\}$ specifies a point in function space, and the random walks step between neighbouring function space points.

The function space lattice for $N = 2$ space points is shown schematically in fig. 5.

Suppose that we start the random walk at some initial function $\phi^{(i)} = (\phi_1, \phi_2 \ldots \phi_N)$ at time τ_i. From there we may step to any one of the $2N$ "nearest neighbour" functions given by $(\phi_1 \pm h_\phi, \phi_2 \ldots \phi_N), (\phi_1, \phi_2 \pm h_\phi \ldots \phi_N) \ldots (\phi_1, \phi_2 \ldots \phi_N \pm h_\phi)$. The choice of which of the N coordinates $\{\phi_j\}$ to increment and whether to increment by $+h_\phi$ or $-h_\phi$ is taken at random.

* Where there is some possibility of confusion we will indicate functionals by putting their arguments within square brackets.

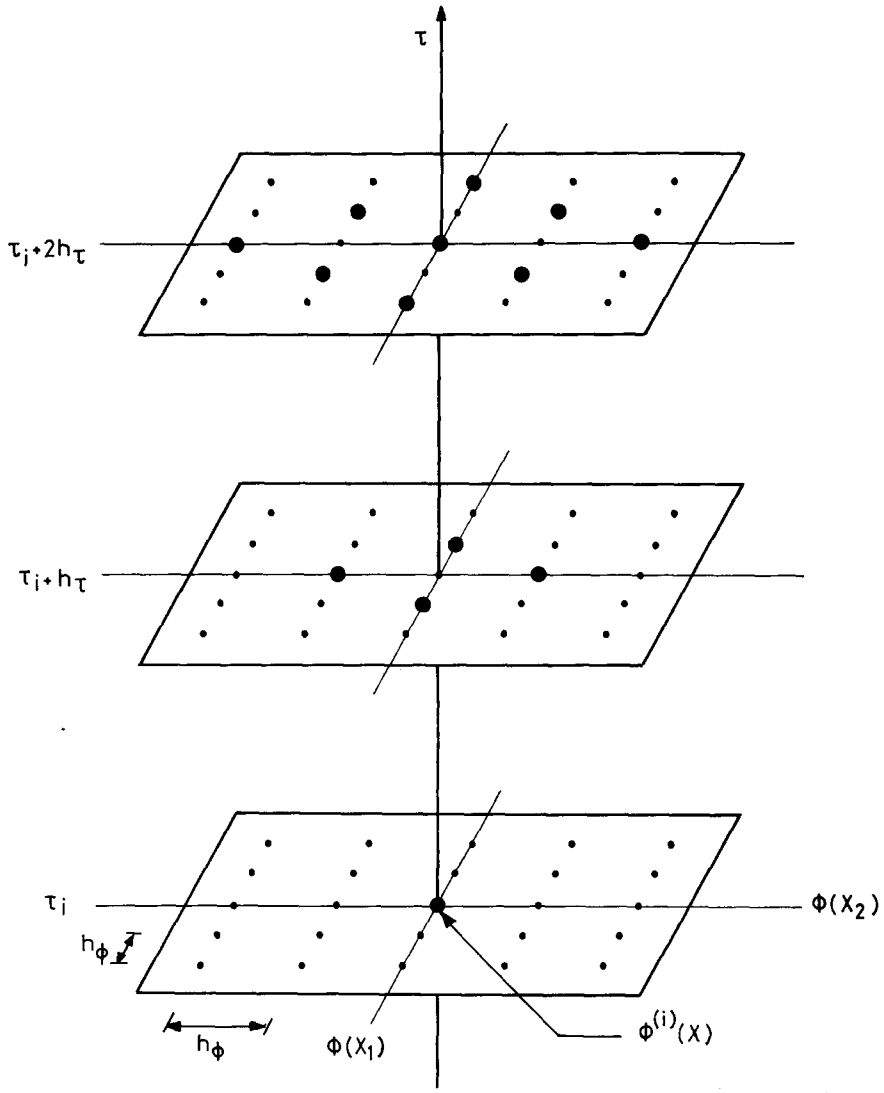

Fig. 5. The (ϕ, τ) function space lattice for $N = 2$. Sites which may be occupied in the first two time steps are indicated.

The probability that the random walk occupies a given site (ϕ, τ) satisfies a generalization of (2.4):

$$p(\phi_1 \ldots \phi_N, \tau + h_\tau) = \frac{1}{2N}\big(p(\phi_1 + h_\phi \ldots \phi_N, \tau) + p(\phi_1 - h_\phi \ldots \phi_N, \tau) + \cdots + p(\phi_1 \ldots \phi_N - h_\phi, \tau)\big). \tag{3.4}$$

In the continuous ϕ-limit with fixed N this becomes

$$-\frac{\partial p[\phi,\tau]}{\partial \tau} = -\frac{1}{2}\frac{h_\phi^2}{Nh_\tau}\sum_{j=1}^{N}\frac{\partial^2}{\partial \phi_j^2}p[\phi,\tau]. \tag{3.5}$$

We can identify $p(\phi,\tau)$ with the wave functional $\psi(\phi,\tau)$ in (3.3) provided we relate the x, ϕ and τ lattice spacings in (3.3) and (3.5) through

$$h_\tau = h_\phi^2 \nu/N. \tag{3.6}$$

Apart from the appearance of the x-space unit cell size ν, this is equivalent to the $h_\tau = h_x^2$ relation found in (2.5) in quantum mechanics. Here, the single degree of freedom in (2.5) has become the N field variables $\{\phi_1 \ldots \phi_N\}$ in the Schrödinger equation (3.2).

To introduce a potential $V(\phi)$ as in (3.2), we must admit the possibility of absorbing the function space random walks. We assume the random walk which has reached some function $\phi(x)$ in fig. 5 has a probability $a[\phi]$ of being absorbed before proceeding to $\tau + h_\tau$. This generalizes the recursion relation (3.4) to

$$p(\phi_1 \ldots \phi_N, \tau + h_\tau) = (1 - a(\phi_1 \ldots \phi_N))\frac{1}{2N}\big(p(\phi_1 + h_\phi \ldots \phi_N, \tau) + \cdots + p(\phi_1 \ldots \phi_N - h_\phi, \tau)\big), \tag{3.7}$$

which has the continuous ϕ-limit

$$-\frac{\partial p[\phi,\tau]}{\partial \tau} = -\frac{1}{2}\frac{h_\phi^2}{Nh_\tau}\sum_{j=1}^{N}\frac{\partial^2}{\partial \phi_j^2}p[\phi,\tau] + \frac{a[\phi]}{h_\tau}p[\phi,\tau]. \tag{3.8}$$

To complete the identification of the random walk probability distribution $p(\phi,\tau)$ and the field theory wave functional in (3.3), we must absorb walks before each time step with the probability

$$a[\phi] = h_\tau \nu \sum_{j=1}^{N} V(\phi)_j. \tag{3.9}$$

Just as in the quantum mechanical example of sect. 2, we may calculate the vacuum energy of a lattice field theory (the zero-point energy) by running random walks from an arbitrary starting function $\phi^{(i)}$ at $\tau_i = 0$ and measuring the number of survivals at some large time τ. This application relies on the result

$$\lim_{\tau \to \infty} p[\phi(x),\tau] = c_0 e^{-E_0 \tau}\psi_0[\phi(x)] \tag{3.10}$$

by analogy with (2.13). We may also separate the vacuum state $\psi_0[\phi(x)]$ or $|\psi_0[\phi(x)]|^2$ for use in the evaluation of Green functions and other matrix elements.

3.2. A STATISTICS PROBLEM AND ITS RESOLUTION: CREATION OF WALKS

Unfortunately, the naive use of absorbing random walks as described above is not practical in field theory. Due to the large number of degrees of freedom, essentially all of the N_0 initial walks are absorbed before we reach the equilibration time τ_e. It is thus impossible to evaluate energies or matrix elements on large lattices by absorbing random walks.

To illustrate this problem, consider a free scalar field theory on the lattice. For simplicity we shall drop the $\frac{1}{2}(\nabla\phi)^2$ term in the classical energy density $V(\phi)$, so the Schrödinger equation (3.3) reduces to a trivial one in N degrees of freedom:

$$-\frac{\partial\psi[\phi,\tau]}{\partial\tau} = \sum_{j=1}^{N}\left(-\frac{1}{\nu}\frac{1}{2}\frac{\partial^2}{\partial\phi_j^2} + \nu\tfrac{1}{2}m_0^2\phi_j^2\right)\psi[\phi,\tau]. \tag{3.11}$$

The energy of an n-particle state in this model is given by

$$E_n = nm_0 + \tfrac{1}{2}Nm_0. \tag{3.12}$$

Now suppose we wish to calculate the zero-point energy to a relative accuracy of $\delta E_0/E_0 = 0.01$ by running random walks in function space from some arbitrary initial function. From the results of sect. 2 (2.20), we would require an initial number N_0 of random walks given by

$$N_0 \sim (10^2)^{2+E_0/(E_x-E_0)} \sim 10^{4+N/2}. \tag{3.13}$$

This is prohibitively large for values of N greater than a small integer. The source of the problem is the proximity of E_m to E_0 on the scale of E_0. To eliminate contamination of the vacuum state by excited states, we must run the random walks to times τ which are much larger than $\tau_e = (E_m - E_0)^{-1}$. Unfortunately, E_0 is generally large relative to $(E_m - E_0)$ for large N. As the number of survivals decays as $e^{-E_0\tau}$, only a tiny fraction of the initial walks, of order $e^{-E_0/(E_m-E_0)}$, survives to $\tau = \tau_e$ to produce the asymptotic $\psi_0[\phi]$ equilibrium distribution.

Fortunately, a simple device allows us to circumvent this problem. We have tacitly assumed that the classical energy density $V(\phi)$ is non-negative, so that the random walk absorption probability $a[\phi]$ in (3.9) is also non-negative. Suppose that we now shift $V(\phi)$ by a constant, so that $a[\phi]$ becomes

$$a[\phi] = h_\tau\left(\nu\sum_{j=1}^{N}V(\phi)_j - E_s\right). \tag{3.14}$$

If $a[\phi]$ is >0 this is still interpreted as the probability per time step of absorbing the random walk. *If $a[\phi]<0$, we introduce the option of creating a new, independent random walk, which branches from the original one at $\phi(x),\tau$.* The probability of creating a new branch at $\phi(x)$ is taken to be $-a[\phi]$.

If we choose $E_s > E_0$, new walks will on average be created in the $a[\phi]<0$ region faster than they are absorbed in the $a[\phi]>0$ region, and the total number of walks at some large time τ will grow as

$$N_\tau \sim N_0 e^{(E_s - E_0)\tau}. \tag{3.15}$$

Creation of random walks in this fashion avoids the statistics problem illustrated by (3.13). It remains necessary to evolve the tree of random walks to a time τ sufficiently large to eliminate contamination of the vacuum by higher excited states, as described in subsect. 2.2. Having done this, the only remaining differences between the random walk results for energies and matrix elements and the continuum results will be due to the restrictions of finite lattice size, limited resolution (h_ϕ, h_x) and limited statistics.

3.3. GENERATION OF $|\psi_0[\phi(x)]|^2$ AND EVALUATION OF FIELD THEORETIC GREEN FUNCTIONS

To evaluate matrix elements such as the equal-time two-point function*,

$$G(x) = \langle 0|\Phi(x,0)\Phi(\mathbf{0},0)|0\rangle = \int \mathrm{D}\phi\, |\psi_0[\phi(x)]|^2 \phi(x)\phi(\mathbf{0}), \tag{3.16}$$

random walks are used to generate a set of classical fields (configurations), $\{\phi^{(n)}(x), n = 1 \ldots N_c\}$, with a $|\psi_0[\phi(x)]|^2$ distribution. The required matrix element, for example $G(x)$, is calculated as an average over the N_c configurations generated:

$$G(x) = \frac{1}{N_c} \sum_{n=1}^{N_c} \phi^{(n)}(x)\phi^{(n)}(\mathbf{0}). \tag{3.17}$$

In practice one may calculate autocorrelations; this non-essential step improves the statistics by $\sqrt{N}$.

$$G(x) = \frac{1}{N_c} \sum_{n=1}^{N_c} \left\{ \frac{1}{N} \sum_{j=1}^{N} \phi^{(n)}(x + y_j)\phi^{(n)}(y_j) \right\}. \tag{3.18}$$

To generate the required configurations $\{\phi^{(n)}(x)\}$, we use a straightforward modification of the quantum mechanical procedure described in sect. 2.3 which

* We use capital Φ's to represent operators and small ϕ's to represent ordinary functions.

produced x points with a $|\psi_0(x)|^2$ distribution. First, we evolve an initial classical function on the function space lattice (fig. 5) to a time $\tau_1 \gtrsim \tau_e$, and record each of the N_1 arrival points $\{\phi^{(m)}(x), m = 1 \ldots N_1\}$ of the branches of the initial function. Each of these arrival points is then used as the starting function of a new tree of random walks, which we evolve until a later time $\tau_2 \gtrsim \tau_1 + \tau_e$. The number of branches b_m which develop from each of the N_1 starting functions $\{\phi^{(m)}(x)\}$ and

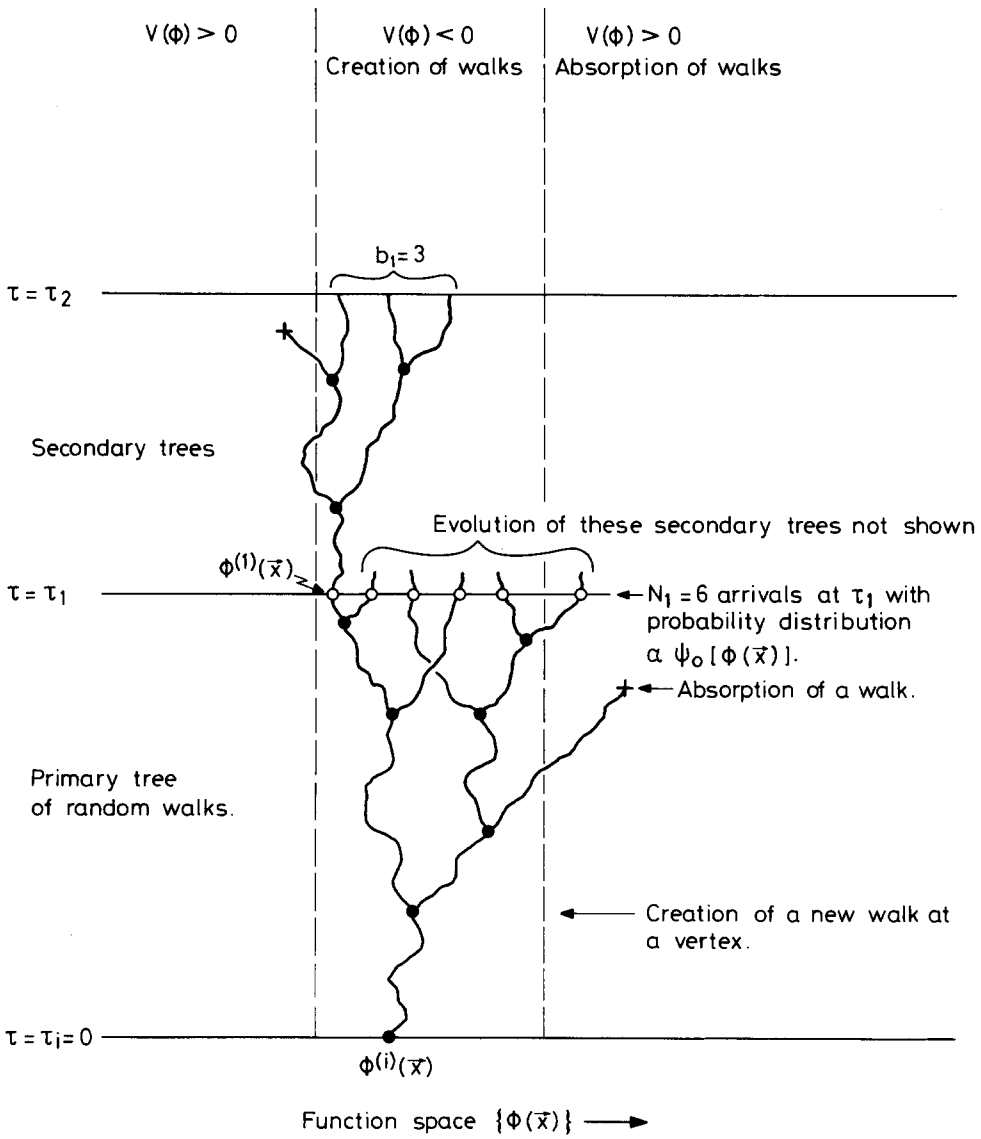

Fig. 6. Schematic evolution of a "tree of trees" of random walks.

survive to τ_2 is then recorded. The evolution of such a tree of random walks is illustrated schematically in fig. 6. Finally, the required matrix element, such as (3.17), is evaluated using the set of configurations $\{\phi^{(m)}(x)\}$ which arrived at τ_1, with the caveat that the contribution of each of the $\{\phi^{(m)}(x)\}$ is counted b_m times; the effective number of configurations is $N_c = \sum_{m=1}^{N_1} b_m$. This procedure produces a set of configurations $\{\phi^{(n)}(x), n = 1 \ldots N_c\}$ with the distribution $|\psi_0[\phi(x)]|^2$ required to evaluate vacuum matrix elements.

3.4. COMPUTATIONAL STRATEGIES

Two alternative ways of implementing this calculation are feasible. In the first the configurations where a new walk is created are preserved in a queue. When a walk terminates, either through being absorbed or through reaching time τ_1 or τ_2 or a preset intermediate time, the calculation is continued at the earliest branch to have been created. A disadvantage of this method is that the length of the queue may grow excessively if the shift in energy E_s is too large. Under these conditions some of the branches, chosen at random, are deleted.

In the second implementation the configurations at the times of creation are copied onto a stack. When the current walk terminates the calculation is resumed at the most recent branch to have been created. The storage requirements are less in this method. It is however inefficient, in that an initial configuration with zero classical energy leads to the rapid creation of walks and these early branches may never be followed. We have used both these methods successfully and it is clear that neither has an overwhelming advantage, although the second is easier to code.

There are two important potential computational advantages of the random walk approach. The computer storage required for a field configuration is reduced over conventional Monte Carlo methods since the field configurations, as they evolve in euclidean time, are generated sequentially rather than simultaneously. This gain is offset by the need to store configurations when branches are created, but our experiments suggest that it is possible to make an overall saving in storage.

A second advantage is that field variables take discrete values and the calculation of the steps of the walk can be accomplished using fast integer arithmetic.

4. Applications

In this section we describe three applications of random walks to model scalar theories in one space dimension. First, we show how mass gaps may be estimated from the equal-time two-point function $G(n)$, and we apply this procedure to the free scalar theory and the model $\lambda{:}(\phi^6 - \phi^4){:}$. Second, we perform measurements of the magnetization $\langle\phi\rangle$ of these two models. Finally, we show how random walks may be used to generate classical solutions in certain cases, and reproduce classical solutions of the free theory as vacuum expectation values of the quantum field ϕ. The random walk parameters used in this section are given in table 1.

TABLE 1
Random walk parameters used in sect. 4

τ_1	$\tau_2 - \tau_1$	N	h_x	h_ϕ	N_b	N_{rw}	Figure
6.0	2.0	9; 2	0.5; 2.0	0.5; 0.25	50	46; 100	7; 8
6.0	2.0	2	2.0	0.25	50	100	9
12.0	2.0	11 (8 active)	1.0	0.25	50	~ 16	10

The integers N_b and N_{rw} are respectively the maximum number of branches allowed in memory, and the number of random walk evaluations averaged to produce each data point.

4.1. EVALUATION OF THE MASS GAP USING RANDOM WALKS

To measure the mass gap, we first determine the equal-time two-point function $G(x)$ using (3.18). This Green function for a free massive scalar theory in one space dimension is given by

$$G(x_n = nh_x|m) = \frac{1}{2Nh_x} \sum_{l=1}^{N} \frac{e^{2\pi i l n/N}}{\sqrt{m^2 + (4/h_x^2)\sin^2(\pi l/N)}} . \tag{4.1}$$

Mass gaps may be estimated by comparing an experimentally determined $G(n)$ with this free theory result. There are clearly many ways to carry out such a comparison. After testing several methods, we have chosen to calculate the *median* $G(n)$ for each n from a histogram of values obtained from many random walk evaluations. This procedure reduces errors due to the large fluctuations although it introduces a systematic error if the distribution is asymmetric. There is clearly scope for replacing the arithmetic average by an improved estimate of the mean, even in conventional Monte Carlo calculations. The estimated mass gap is then determined from a least squares fit of the median Green function $G^{med}(n)$ to the free theory $G(n|m)$, with the mass m taken as a parameter. A typical numerically evaluated median Green function for the free, massive scalar theory is shown in fig. 7, together with the exact theoretical result (4.1). This median Green function is determined from a histogram of 46 random walk Green functions, and required a total of 560 CPU sec on an IBM3081 to evaluate. A least squares fit of this $G^{med}(n)$ to (4.1) gives an estimated mass gap of $m^{(est)} = 0.957$, whereas the actual input mass is $m = 1.0$.

To illustrate the evaluation of the mass gap of a nontrivial theory, we turn to the $\phi^6 - \phi^4$ model of Glimm, Jaffe and Spencer [12] which is described by the potential

$$V(\phi) = \tfrac{1}{2}(\nabla\phi)^2 + :\lambda(\phi^6 - \phi^4) + \tfrac{1}{2}m_0^2\phi^2:_{m_0} . \tag{4.2}$$

Numerical results for the mass gap m/m_0 as a function of λ/m_0^2 on an $N = 2$ lattice

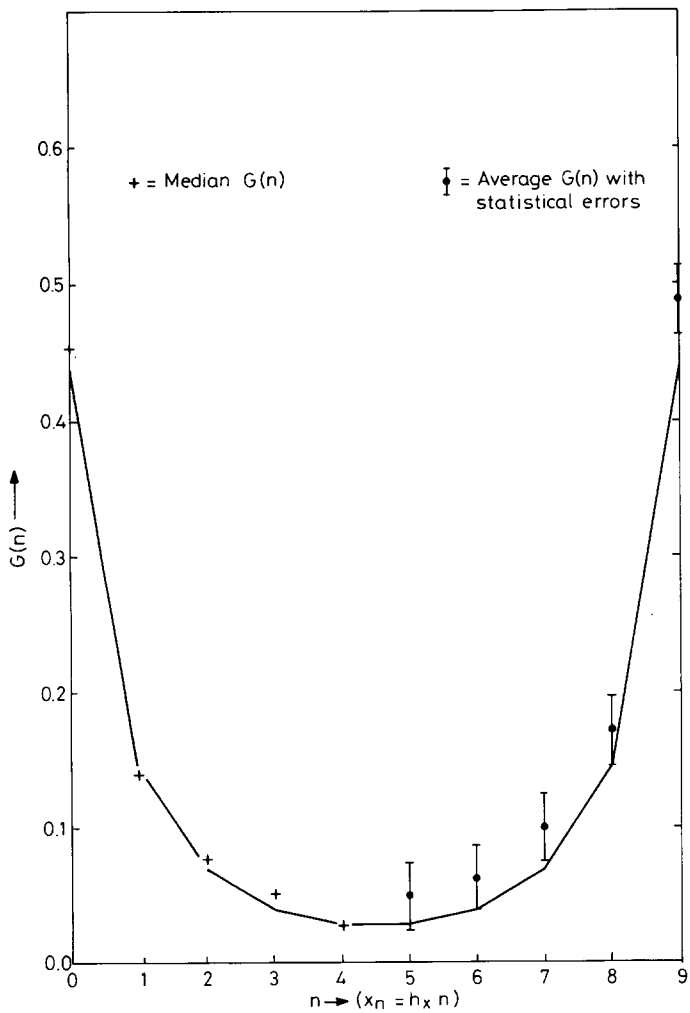

Fig. 7. Random walk evaluation of the two-point function $G(n)$ for a free scalar theory. The solid curve is the exact result.

are implicit in table 1 of ref. [13]. These and a few additional unpublished points for the $\phi^6 - \phi^4$ mass gap are shown in fig. 8, together with random walk results obtained by least squares fits of median Green functions to (4.1). Each median Green function is determined from 100 random walk evaluations of $G(n)$, requiring approximately 200 CPU sec. Deviation of m(random walk) from m(hamiltonian) for $m/m_0 \lesssim 0.3$ is due to noise in the random walk $G^{\text{med}}(n)$. As $m \to 0$ implies a constant $G(n)$, any noise in $G^{\text{med}}(n)$ produces a spurious apparent mass, which is $\sim 0.1 m_0$ with these random walk parameters. Obviously this noise level may be reduced through improved statistics.

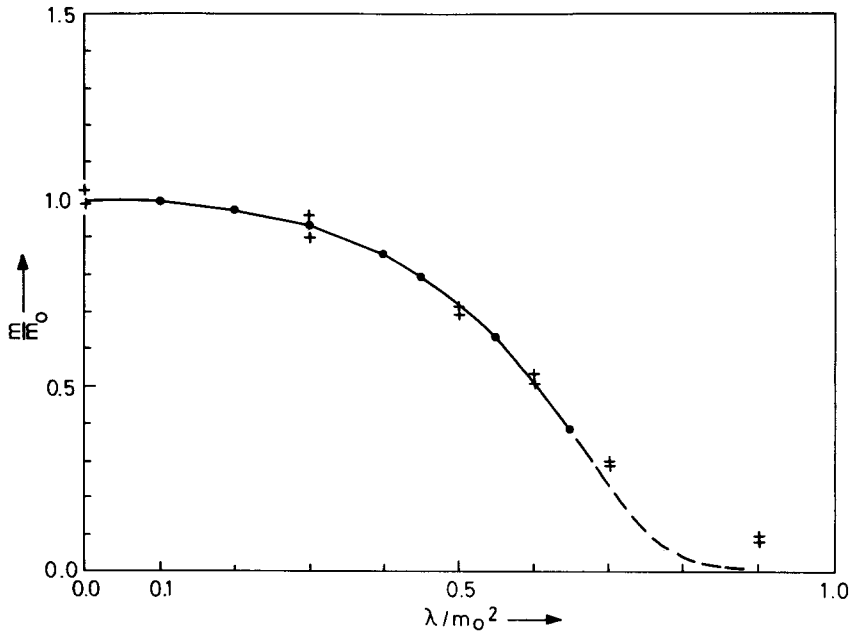

Fig. 8. The mass gap $m/m_0(\lambda/m_0^2)$ in $\lambda{:}(\phi^6-\phi^4)_2{:}$. The dots (•) show values summarized in [13], and the crosses (+) show two independent random walk measurements.

4.2. MAGNETIZATION MEASUREMENTS

The magnetization $\langle\phi\rangle$ in the presence of an external source $H=-h\phi$ may be evaluated using random walks, through the general procedure for calculating matrix elements described in subsect. 3.3. The dependence of $\langle\phi\rangle$ on h is of special interest in the study of phase transitions, as $\langle\phi(h)\rangle$ may have singular h-dependence at a critical point. Here we shall evaluate the magnetization $\langle\phi\rangle$ obtained in a free scalar theory of unit mass as a function of h; $V(\phi)$ is given by

$$V(\phi)=\tfrac{1}{2}(\nabla\phi)^2+\tfrac{1}{2}m^2\phi^2-h\phi, \tag{4.3}$$

and the expected magnetization is

$$\langle\phi\rangle\equiv\frac{1}{N}\left\langle\sum_{j=1}^{N}\phi(x_j)\right\rangle=h/m^2. \tag{4.4}$$

The result of a random walk evaluation of $\langle\phi(h)\rangle$ in the free theory (4.3) with $m=1$ is shown in fig. 9. Here we have calculated the average $\langle\phi\rangle$ rather than the median, as the median and average $\langle\phi\rangle$ values are very similar. The lattice parameters used in this example are the same as in the $(\phi^6-\phi^4)$ mass gap evaluation.

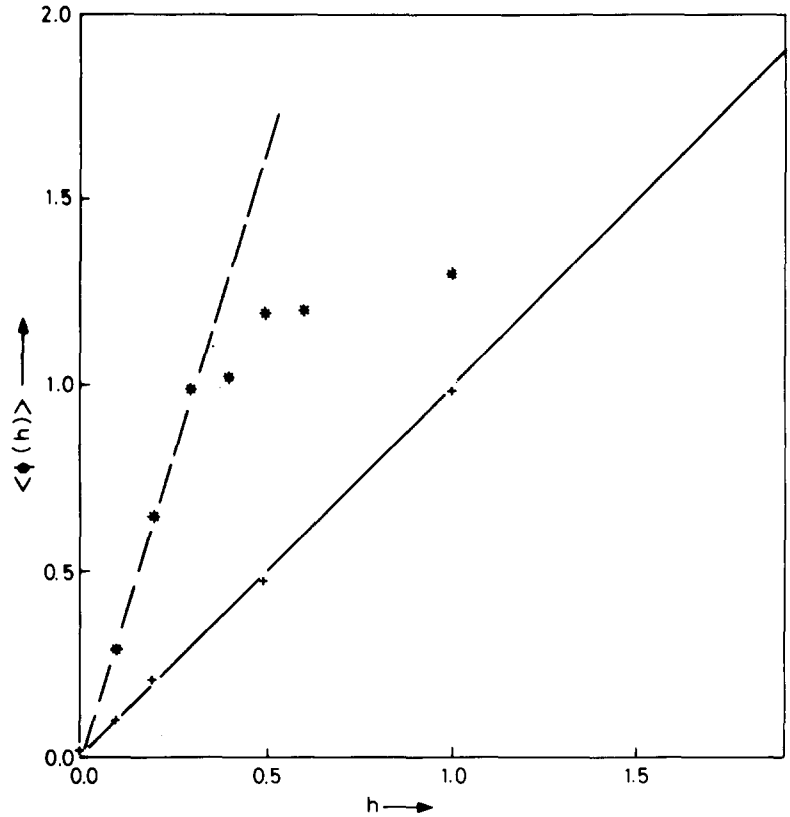

Fig. 9. Magnetization curves $\langle\phi(h)\rangle$ for the free massive theory (+) and for $\lambda{:}(\phi^6-\phi^4)_2$: with $\lambda = 0.6(*)$.

For purposes of comparison we also show the magnetization $\langle\phi(h)\rangle$ found in the $\lambda{:}(\phi^6-\phi^4)$: model of (4.2). There are two features of this magnetization curve which are of special interest. One is the zero-field susceptibility

$$\chi(0) = \left.\frac{\mathrm{d}\langle\phi(h)\rangle}{\mathrm{d}h}\right|_{h=0} = \frac{1}{m^2} \sim 3.4, \tag{4.5}$$

which gives a mass gap of

$$m \sim 0.55. \tag{4.6}$$

This is consistent with the median Green function estimate of $m \sim 0.52$ in fig. 8. Second, we note the expected saturation of the model above $\langle\phi\rangle \sim 1$, due to the rapid rise of the $\lambda\phi^6$ term in $V(\phi)$.

The phase transition ($m \to 0$) expected in this model can presumably be studied by evaluating $\langle\phi(h)\rangle$ on larger and finer lattices; the limitation here in one space dimension is CPU time rather than storage requirements.

4.3. RECOVERY OF CLASSICAL SOLUTIONS

At least in the free theory case one may recover solutions $\phi_c(x)$ of the classical field equations as the expectation value of the fluctuating quantum field $\phi(x)$ in the vacuum state $\psi_0[\phi(x)]$. This is so because the presence of a static external source in the hamiltonian of the free theory

$$H_I = -\int dx h(x)\phi(x) \tag{4.7}$$

simply results in a shift of $\phi(x)$ in the vacuum state. The new vacuum is a coherent state; explicitly, it is

$$\psi_0[\phi(x)] = \eta \exp\left\{-\tfrac{1}{2}\int dx\,(\phi(x)-\phi_c(x))\sqrt{m_0^2-\nabla^2}\,(\phi(x)-\phi_c(x))\right\}. \tag{4.8}$$

The displacement $\phi_c(x)$ by substitution into the generalization of (3.2) can be seen to satisfy the classical field equation

$$(m_0^2-\nabla^2)\phi_c(x) = h(x), \tag{4.9}$$

and the expectation value of $\phi(x)$ in the vacuum state (4.8) is obviously ϕ_c:

$$\langle\phi(x)\rangle = \int D\phi\,|\psi_0|^2\phi(x) = \phi_c(x). \tag{4.10}$$

To obtain nontrivial examples of $\langle\phi(x)\rangle$ in the free theory, we impose boundary conditions on the field ϕ at specified x-sites. In particular, we choose $\phi(x=\pm 5.0) = \mp 2.0$ and $\phi(x=0.0)=0$. This is equivalent to a generalization of (4.7) to a quadratic external source

$$H_I = \int dx\left(-h(x)\phi(x)+\tfrac{1}{2}\sigma(x)\phi(x)^2\right), \tag{4.11}$$

with singular sources at the boundary points. The classical field result (4.10) on which this application rests remains valid assuming (4.11).

The expectation values of $\phi(x)$ in the free scalar theory with these boundary conditions as determined using random walks are shown in fig. 10, for massless and massive ($m=1.0$) cases. The corresponding classical solutions which we show as solid lines are

$$\phi_c(x) = \begin{cases} -0.4x, & m=0 \\ -\dfrac{2}{\sinh 5}\sinh x, & m=1. \end{cases} \tag{4.12}$$

Agreement between these curves and the numerical results is satisfactory.

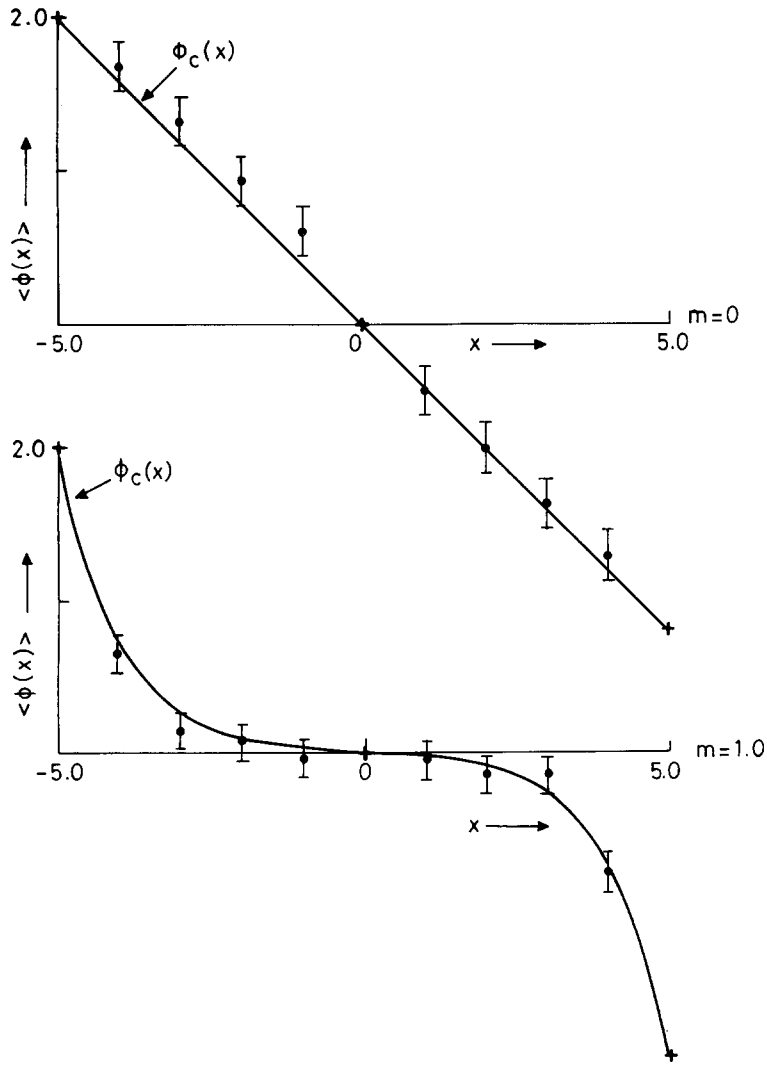

Fig. 10. Vacuum expectation values of $\phi(x)$ generated using random walks (⊕) and the corresponding classical solution $\phi_c(x)$. The + points are boundary conditions.

These classical solutions represent the average of ~ 16 random walk evaluations of $\langle\phi(x)\rangle$; each curve required ~ 200 CPU sec. This application required a rather large value of run time τ_1 for the initial tree to reach an equilibrium distribution, probably because $\langle\phi(x)\rangle$ is far from the starting function $\phi^{(i)} = (2.0, 0.0, 0.0 \ldots 0.0, -2.)$. The results shown are for $\tau_1 = 12$, twice the value we have used elsewhere.

5. Conclusions and future developments

We have shown how field theoretic vacuum expectation values may be evaluated numerically using random walks in function space. The random walks simulate a diffusion process, which is described by the Schrödinger equation in euclidean time in the continuum limit. A technique which produces configurations at a fixed time with a $|\psi_0[\phi(x)]|^2$ distribution is described; using this technique, vacuum expectation values may be measured directly.

In this paper we develop a method in which branches of the initial random walk are created or absorbed with a probability proportional to their classical energy. This method is applied to scalar theories in one space dimension, and we demonstrate the evaluation of mass gaps, the magnetization $\langle\phi\rangle$ and classical solutions; the numbers we find are consistent with known results.

There are two interesting future developments of random walk techniques which we anticipate. First, the possibility of extending this method to gauge theories (the required lattice Schrödinger equation for $\psi[U(x)]$ analogous to our eq. (3.2) is given in [14]) and fermions is an area of obvious interest. Fermion random walks are especially attractive as a possible method for avoiding the quenched approximation. Second, it is possible to solve the functional Schrödinger equation (3.2) by guiding the walk direction, without creating and absorbing branches as we have done in this paper. The guiding option requires the storage of only a single configuration and is much faster than branching [15], hence we expect that guided random walks may prove more practical on large lattices or in three space dimensions.

We are indebted to A. Jaffe and D. Storey for a number of useful conversations and to D. Storey for a reading of the manuscript. The support of the Theory Group, HEP Division, Rutherford Appleton Laboratory and the Physics Department of the University of Southampton in the course of this work is gratefully acknowledged.

References

[1] M.H. Kalos, Phys. Rev. 128 (1962) 1791
[2] M.H. Kalos, J. Comp. Phys. 2 (1967) 257; Phys. Rev. A2 (1970) 250
[3] M.H. Kalos, D. Levesque and L. Verlet, Phys. Rev. A9 (1974) 2178
[4] D.W. Heys and D.R. Stump, Phys. Rev. D28 (1983) 2067; D29 (1984) 1784, 1791; Phys. Rev. D30 (1984) 1315
[5] B.D. Serot, S.E. Koonin and J.W. Negele, Phys. Rev. C28 (1983) 1679;
S.A. Chin, J.W. Negele and S.E. Koonin, Ann. of Phys. 157 (1984) 140
[6] R. Blankenbecler and R.L. Sugar, Phys. Rev. D27 (1983) 1304
[7] J. Ranft and A. Schiller, CERN-TH-3784 (1983) and references cited therein
[8] M. Creutz and B. Freedman, Ann. of Phys. 132 (1981) 427
[9] R.P. Feynman and A.R. Hibbs, Quantum mechanics and path integrals (McGraw-Hill, 1965) 193
[10] E. Fermi, in N. Metropolis and S. Ulam, J. Am. Stat. Assoc. 247 (1949) 335

[11] T. Barnes and G.J. Daniell, Phys. Rev. D28 (1983) 2045, and references cited therein
[12] J. Glimm, A. Jaffe and T. Spencer, Proc. Ettore Majorana, School of Mathematical Physics (Springer, 1973) 165
[13] T. Barnes and G.J. Daniell, Phys. Lett. 142B (1984) 188
[14] J.P. Greensite, Nucl. Phys. B166 (1980) 113
[15] T. Barnes, G.J. Daniell and D. Storey, Rutherford/Southampton/Toronto preprint RAL-85-004/SHEP-84-85-4/UTPT-85-01 (January 1985)